

# Substrate Integrated Waveguides Optimized for Ultrahigh-Speed Digital Interconnects

Jamesina J. Simpson, *Student Member, IEEE*, Allen Taflove, *Fellow, IEEE*, Jason A. Mix, and Howard Heck, *Member, IEEE*

**Abstract**—This paper reports an experimental and computational study of substrate integrated waveguides (SIWs) optimized for use as ultrahigh-speed bandpass waveguiding digital interconnects. The novelty of this study resides in our successful design, fabrication, and testing of low-loss SIWs that achieve 100% relative bandwidths via optimal excitation of the dominant  $TE_{10}$  mode and avoidance of the excitation of the  $TE_{20}$  mode. Furthermore, our optimal structures maintain their 100% relative bandwidth while transmitting around  $45^\circ$  and  $90^\circ$  bends, and achieve measured crosstalk of better than  $-30$  dB over the entire passband. We consider SIWs operating at center frequencies of 50 GHz, accommodating in principle data rates of greater than 50 Gb/s. These SIWs are 35% narrower in the transverse direction and provide a 20% larger relative bandwidth than our previously reported electromagnetic bandgap waveguiding digital interconnects. Since existing circuit-board technology permits dimensional reductions of the SIWs by yet another factor of 4:1 relative to the ones discussed here, bandpass operation at center frequencies approaching 200 GHz with data rates of 200 Gb/s are feasible. These data rates meet or exceed those expected eventually for proposed silicon photonic technologies.

**Index Terms**—Finite-difference time-domain (FDTD) methods, multiprocessor interconnection, waveguide bends, waveguides.

## I. INTRODUCTION

SINCE THE advent of digital computers in the 1940s, baseband metallic stripline circuit-board interconnects have been employed for transmitting data between processors. Until recently, such interconnects provided adequate bandwidths even while data rates increased according to Moore's Law [1]. However, as clock speeds continue to rise in the microwave frequency range above 3 GHz, problems with signal integrity, cross-coupling, and radiation that are intrinsic to stripline interconnects are becoming increasingly difficult to overcome. This has led to significant research in silicon photonics [2], which would replace the metallic striplines with optical fibers. However, realization of the complete suite of required opto-electronic technologies will involve a complex set of tasks to implement a fundamental paradigm shift in chip and interconnect design. This will necessarily involve years of study.

Manuscript received October 31, 2005; revised February 8, 2006. This work was supported by the Intel Corporation and by the National Computational Science Alliance under Grant ECS050007N.

J. J. Simpson and A. Taflove are with the Department of Electrical Engineering and Computer Science, Northwestern University, Evanston, IL 60208 USA (e-mail: j-simpson@northwestern.edu).

J. A. Mix and H. Heck are with the Platform Technologies Laboratory, Intel Corporation, Hillsboro, OR 97124 USA.

Digital Object Identifier 10.1109/TMTT.2006.873622

This paper reports our recent computational and experimental studies which advance an attractive alternate possibility that relies upon evolutionary, rather than revolutionary, developments in interconnect technology. Specifically, we report the successful design, construction, and testing of ultrahigh-speed low-loss low-crosstalk bandpass waveguiding interconnects implemented in conventional circuit boards. While our measurements have been limited, to date, to bandwidths suitable for 50-Gb/s data transmission rates, it is clear that these interconnects can be scaled to permit operation at data rates of 200 Gb/s with no improvements in circuit-board manufacturing techniques. These data rates meet or exceed those expected eventually for proposed silicon photonic technologies.

The optimized bandpass waveguiding interconnects discussed in this paper are based upon the substrate integrated waveguide (SIW) configuration [3]–[9]. Here, a waveguide mode is bounded vertically by two copper planes of a double-sided circuit board, and is bounded transversely by single rows of cylindrical copper pins (vias) electrically bonded to the opposing ground planes. Input and output coupling is achieved using coaxial lines terminated with short vertical probes extending completely across the gap between the upper and lower ground planes. Each probe is electrically isolated from the ground planes by etching oversized holes through the ground planes at the probe locations.

Previously, we reported computational and experimental results for electromagnetic bandgap (EBG) waveguides [10], [11] operating at 10 GHz [12] and 50 GHz [13], [14]. Those structures were similar to SIWs with the exception that each waveguide was bounded in the plane of propagation by double rows of vias. Here, we build upon our EBG waveguide work to show how SIWs can be optimally designed to realize easily constructed compact waveguiding structures suitable for use as ultrahigh-speed waveguiding digital interconnects. Specifically, we show that it is possible to achieve SIWs optimized for narrow transverse dimensions, low loss, low crosstalk, and maximum bandwidth with no multimoding. The novelty of this study resides in our successful design, fabrication, and testing of low-loss SIWs that achieve 100% relative bandwidths via optimal excitation of the dominant  $TE_{10}$  mode and avoidance of the excitation of the  $TE_{20}$  mode. Furthermore, our optimal structures maintain their 100% relative bandwidth while transmitting around  $45^\circ$  and  $90^\circ$  bends, and achieve measured crosstalk of better than  $-30$  dB over the entire passband. Our results indicate that these optimized SIWs should have excellent utility when implemented in modern digital circuit boards having typically dense layouts.

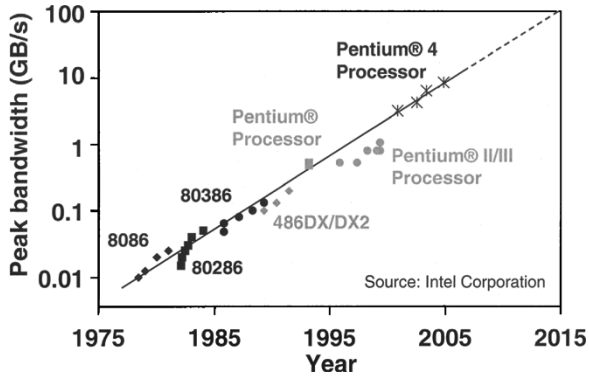


Fig. 1. Host interface bandwidth demand trend for Intel Corporation microprocessors. Peak bandwidth demand has grown at a rate of  $1.66\times$  every two years since 1978.

The remainder of this paper is organized as follows. Section II provides background information relevant to the current study. Section III presents our computational and experimental study of a single straight EBG waveguide embedded in a standard double-sided circuit board comprised of FR4 dielectric and operating at a center frequency of 50 GHz. This study forms the basis of our SIW investigations subsequently reported, and is included for purposes of comparison with these results and to demonstrate the capabilities and accuracy of our finite-difference time-domain (FDTD) [15] models. Section IV presents our new computational and experimental results for an optimized single straight SIW implemented in a double-sided circuit board comprised of Rogers RT/Duroid 5880 dielectric and operating at a 50-GHz center frequency. This section also illustrates FDTD modeling results for an SIW structure scaled to a center frequency of 130 GHz. Section V then presents our new computational and experimental results for crosstalk between adjacent SIWs, and Section VI reports FDTD modeling results for optimized  $45^\circ$  and  $90^\circ$  SIW bends that are capable of maintaining the ultrawide relative bandwidth of  $\sim 100\%$ . Finally, Section VII concludes the paper and presents details of our ongoing research in this area.

## II. BACKGROUND AND SUMMARY OF OUR PREVIOUS RESEARCH

Since the birth of the personal computer, Moore's Law [1] has had great success in predicting the performance growth of microprocessors and PC systems. Using such metrics as processor frequency and millions-of-instruction per second (MIPs), the trends show exponential growth, with a doubling in performance roughly every 18–24 months [16].

Fig. 1 represents the assessment by Intel Corporation, Santa Clara, CA, of how such exponential performance growth also applies to rates of inter-chip data transmission. Contemporary host interface designs employ an 8-B-wide data bus operating at 1.066 Gb/s with a bi-directional single-ended signal to provide a peak bandwidth of  $\sim 8.5$  GB/s. Extrapolating the trend in this figure, we predict a bandwidth demand of more than 100 GB/s within ten years, which requires increasing the width of the interface, increasing the per signal data rate, or a combination of the two. In the cost-driven environment of the PC market place,

typical desktop PCs use low cost four-layer FR4-based motherboards. Increasing the width of the host interface drives higher cost by requiring additional layers in the motherboard, making wider interfaces unattractive.

Addressing the demand via scaling to higher data rates presents difficulties as well. Multigigabit/s signaling solutions typically employ differential unidirectional signaling, which limits the data bus width to 2 B in order to fit within a four-layer motherboard. Under these conditions, the data rate demand becomes 50 Gb/s per differential pair, a requirement that exceeds the expected capability of printed circuit board (PCB)-based transmission line signaling by a factor of 2 [17].

Anticipating this difficulty in meeting the projected bandwidth demand of future microprocessors, we have conducted an investigation of alternative waveguiding structures that have the promise of mitigating or even avoiding the problems associated with conventional metallic interconnects, and yet can be implemented using standard circuit board fabrication techniques. Specifically, as reported in [12], our initial proof-of-concept research implemented EBG waveguides in standard PCBs. This resulted in a measured passband extending from 6 to 14.1 GHz with an insertion loss over the passband ranging from 3.6 to 7.3 dB.

Success in this initial proof-of-concept led us to investigate the scalability of the EBG structure to a 50-GHz center frequency, as initially reported in [13] and [14]. Our motivation here was twofold. First, the dimensions of EBG structures scale inversely with frequency, reducing the transverse width of the EBG waveguide structure. Second, the higher center frequency is required in order to achieve higher data transmission rates. Section III expands upon the research reported in [13] and [14] by implementing a 14-pole Debye model for the FR4 dielectric dispersion characteristic at a 50-GHz center frequency.

## III. SINGLE STRAIGHT EBG INTERCONNECT WITH 80% RELATIVE BANDWIDTH

Our computational and experimental study of a single straight EBG waveguide embedded in a standard double-sided circuit board comprised of an FR4 dielectric and operating at a center frequency of 50 GHz is presented here. This study forms the basis of our SIW investigations to be subsequently presented, and is included for purposes of comparison with these results and to demonstrate the capabilities and accuracy of our FDTD models.

We first show results for an EBG waveguide analogous to those described in [12]–[14]. As in [12]–[14], the EBG waveguide is formed by removing two rows of a square lattice of pins having initially six rows. We also use the same pin radius to center-to-center spacing ratio ( $r/a = 18\%$ ) and pin radius to waveguide width ratio ( $r/w = 6\%$ ). In the current study, however, the EBG structure is scaled to a center frequency of 50 GHz and uses FR4 as the dielectric material ( $\epsilon_r \sim 3.9$  and  $\tan \delta \sim 0.017$  at 50 GHz).

For our FDTD simulations, we use a high-resolution three-dimensional (3-D) grid having a space-cell size of  $4.4 \times 4.4 \times 7 \mu\text{m}$  and a stable time step near the Courant limit. A 14-pole Debye model is implemented to accurately simulate

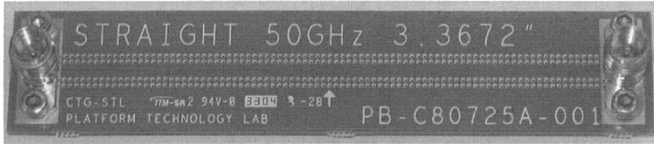


Fig. 2. 8.6-cm-long EBG interconnect scaled to a center frequency of 50 GHz. This test structure is comprised of an FR4 dielectric material ( $\epsilon_r = 3.9$  and  $\tan \delta = 0.017$ ) and has  $r = 0.93$  mm,  $a = 0.17$  mm,  $w = 2.8$  mm, and  $h = 0.76$  mm.

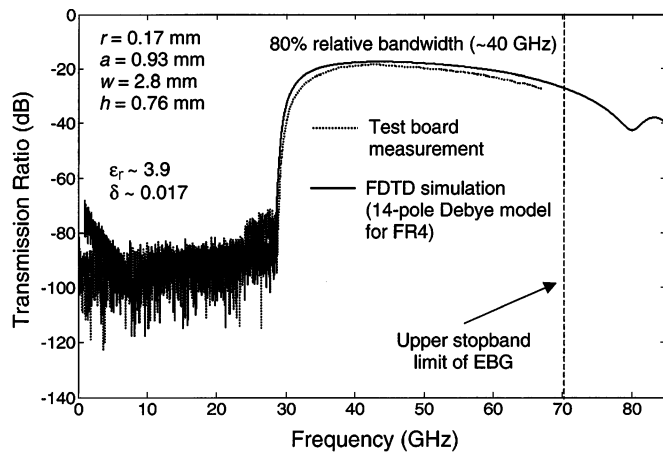


Fig. 3. Comparison between the measured and FDTD-calculated  $S_{21}$  characteristics over the 8.6-cm-long EBG interconnect of Fig. 2.

the dispersive characteristics of the FR4 dielectric. In addition, a frequency-dependent skin-effect model is implemented for all copper surfaces [18]. The waveguide spans approximately 8.6 cm between the input and output probes, has height  $h = 0.76$  mm between the upper and lower ground planes, and distance  $w = 2.8$  mm (center-to-center) between the rows of vias immediately bounding the waveguide. Each via has a radius  $r = 0.17$  mm and is separated from its neighboring via with a center-to-center spacing  $a = 0.93$  mm. Fig. 2 presents a photograph of the corresponding test structure used in the measurements.

Fig. 3 compares the measured and FDTD modeling results for the insertion loss ( $S_{21}$ ) of the 8.6-cm-long structure of Fig. 2. A standard Agilent microwave network analyzer (with capabilities to 67 GHz) having 50- $\Omega$  nominal source and load impedances was used in these measurements. From Fig. 3, we first note that there exists a sharp transition from a deep stopband (below  $-80$  dB) to a passband at approximately 30 GHz. This passband extends to approximately 70 GHz, above which the EBG structure can no longer effectively confine the propagating signal (yielding an upper stopband limit) [12]. This EBG waveguide, therefore, provides an approximately 80% fractional bandwidth.

From Fig. 3, we also note very good agreement between the measured and FDTD-calculated  $S_{21}$  characteristics over a wide dynamic range. This agreement extends all the way to the upper stopband limit of the EBG structure despite the complicated dispersive properties of the FR4 dielectric. At midband (50 GHz),  $S_{21}$  for the 8.6-cm-long EBG waveguide is  $-20.4$  dB. Comparison of this result with that of an identical, but longer (12.7 cm) waveguide indicates that each coaxial

transition introduces an input/output coupling loss of only approximately 0.6 dB. Combined with the flatness of the  $S_{21}$  characteristic in the passband, it is apparent that the simple probes used to excite and receive the waveguide mode provide excellent broadband matching. Since the remaining loss is caused by propagation attenuation in the FR4 dielectric, it is clear that migration of this technology to the millimeter-wave regime will require the use of dielectric materials having low loss up to several hundred gigahertz. Candidate materials for this application include aerogels [19]. For intermediate frequencies, alternative materials such as Rogers RT/Duriod 5880 dielectric may be used, as shown below.

#### IV. SINGLE STRAIGHT SIW INTERCONNECT WITH 100% RELATIVE BANDWIDTH

Our new computational and experimental results for an optimized single straight SIW implemented in a double-sided circuit board comprised of glass reinforced PTFE dielectric, Rogers RT/Duriod 5880, and operating at a 50-GHz center frequency is presented here. In this structure and all others discussed in this paper, which are comprised of this Rogers RT/Duriod 5880 dielectric, comprehensive data for the frequency dependence of the dielectric are not available at this time. As a result, we use a frequency-independent model when simulating the Rogers RT/Duriod 5880 dielectric ( $\epsilon_r = 2.2$ ,  $\tan \delta = 0.0009$ ). This necessarily reduces the agreement between the measured and FDTD results, but not to the point where the computational modeling loses utility.

The EBG interconnect designs of Section III and [12]–[14] employed  $r/a = 18\%$  and  $r/w = 6\%$ , and required at least two rows of pins bounding the waveguide to prevent significant leakage [12]. Since we are interested in designing an interconnect having the smallest possible dimensions transverse to the direction of propagation, we now study waveguides bounded by a single row of pins (i.e., SIWs). This involves numerous simulations for two classes of parametric studies, which are: 1) varying  $a$  while maintaining constant  $r$  and  $w$  and 2) varying  $r$  while maintaining constant  $a$  and  $w$ . From parametric study 1), relative to the EBG waveguides of Section III and [12]–[14], we find that in order to maintain a constant cutoff frequency of the fundamental mode,  $w$  must be increased by up to 8% as  $a$  decreases toward a value of  $2r$  (forming a corrugated waveguide with adjacent pins touching and having zero leakage). Taking this into account, we find that the widest bandwidth is obtained for  $a = 2r$ . From parametric study 2), we find that the optimal  $r/w$  ratio remains 6%. For larger or smaller values of  $r/w$ , the bandwidth is reduced.

Considering the above findings, the design criterion for an optimum SIW interconnect is  $r/w = 6\%$  and  $a = 2r$ . However, having adjacent via pins in contact poses a difficult fabrication problem. Consequently, in the results presented here, we include a small gap of  $0.83r$  (0.20 mm) between adjacent vias. At present, this is approximately the minimum feasible gap size in standard circuit boards. Fig. 4 presents a photograph of an optimized 7.6-cm-long SIW interconnect designed to these specifications. The interconnect is comprised of a low-loss Rogers RT/Duriod 5880 dielectric for the case of  $r = 0.24$  mm,  $a = 0.68$  mm,  $w = 4.1$  mm, and  $h = 0.76$  mm. This SIW is 35%



Fig. 4. 7.6-cm-long SIW interconnect scaled to a center frequency of 50 GHz. This test structure is comprised of Rogers RT/Duriod 5880 dielectric material ( $\epsilon_r = 2.2$  and  $\tan \delta = 0.0009$ ) and has  $r = 0.24$  mm,  $a = 0.68$  mm,  $w = 4.1$  mm, and  $h = 0.76$  mm. Further, it is 35% smaller in the transverse direction than the EBG waveguide of Fig. 2.

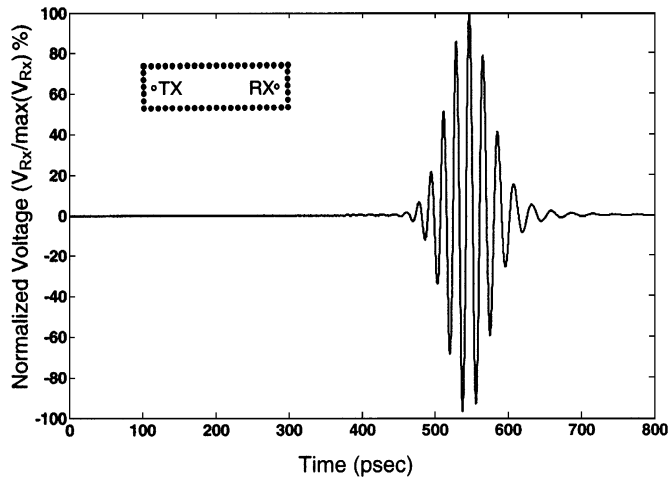


Fig. 5. FDTD-calculated normalized time waveform of the received voltage of the interconnect of Fig. 4 for an assumed 134-ps (full-width at half-maximum) transmitted 50-GHz carrier pulse having a Gaussian envelope.

narrower in the transverse direction than our previously reported EBG interconnects of Section III and [12]–[14].

Fig. 5 shows the FDTD-calculated normalized time waveform of the received voltage of the interconnect of Fig. 4 for an assumed 134-ps (full-width at half-maximum) transmitted 50-GHz carrier pulse having a Gaussian envelope. For this case, the spectrum of the transmitted pulse is centered at 50 GHz and falls to  $-22$  dB at 27 and 81 GHz, respectively, the lower and upper limits of the SIW passband. From Fig. 5, we see that the received pulse exhibits little ringing. In fact, upon overlaying the received and transmitted pulses, we find essential coincidence of the zero-crossings and very little distortion.

Fig. 6 compares the associated spectrum of the measured and FDTD-calculated  $S_{21}$  characteristics for the SIW structure of Fig. 4. From Fig. 6, we observe a deep stopband of better than  $-80$  dB below approximately 27 GHz. Above 27 GHz, the  $S_{21}$  characteristic transitions to an ultrawide passband extending to 81 GHz, providing an approximately 100% bandwidth. The 27-GHz cutoff frequency agrees with that calculated using the equation provided by [5] for the effective width of an equivalent rectangular waveguide

$$w_{\text{eff}} = w - 1.08 \left[ \frac{(2r)^2}{a} \right] + 0.1(2r)^2/w.$$

As previously explained, the deviation of the measured and FDTD results within the passband is caused by the assumption of frequency-independent dielectric properties of the Rogers

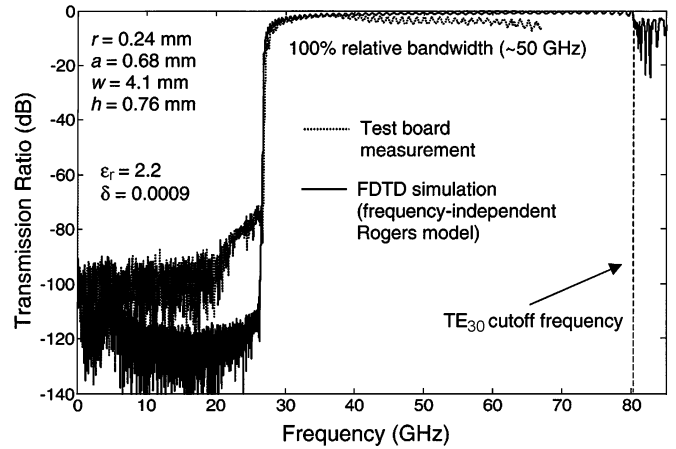


Fig. 6. Comparison between the measured and FDTD-calculated  $S_{21}$  characteristics over the optimized 7.6-cm-long SIW interconnect of Fig. 4.

RT/Duriod 5880 dielectric. The measured midband transmission loss is only 3.6 dB, a value which includes the coupling losses of the two probes and the wave propagation attenuation. Comparison of this result with those of identical, but longer (12.7 and 25.4 cm) waveguides yields 0.31-dB/cm propagation loss in the Rogers RT/Duriod 5880 dielectric at midband.

The  $\sim 100\%$  relative bandwidth seen in Fig. 6 is larger than the  $\sim 80\%$  bandwidths obtained in Section III and [12]–[14] for two reasons, which are: 1) the passband is not bounded by any stopband limit imposed by the bounding vias [12] and, hence, the passband can extend fully to the cutoff frequency of the second even transverse electric (TE) mode and 2) for the case studied here, the transmitting and receiving probes are centered transversely in the waveguide and longitudinally positioned at what appears to be an optimum location of one-quarter wavelength at midband ( $\sim 54$  GHz) from the ends of the waveguide (whereas in Section III and [12]–[14] the probes were positioned inline with the second column of vias). Both of these optimizations are discussed in more detail below.

We now discuss reason 1) for the improved bandwidth of the SIW structures discussed here relative to our previous results. From [5], we know that the TE-mode cutoff frequencies of the SIW are the same as for those of a flat-wall rectangular waveguide having the same effective waveguide width  $w_{\text{eff}}$ . (The SIW considered here has  $w_{\text{eff}} = 3.74$  mm.) Note that TM modes are not supported by the SIW structure [5] and, therefore, need not be considered. Fig. 7 illustrates the results of an investigation to see if odd TE modes can be excited in the SIW, especially the first odd TE mode, which would arise at approximately midband and potentially disrupt the desired fundamental-mode operation of the interconnect. This figure compares the measured  $S_{21}$  characteristics for two 7.6-cm-long SIW interconnects of the type shown in Fig. 4. The first characteristic is for the case of both transmitting and receiving probes at the optimum transverse and longitudinal locations, while the second characteristic is for the case of both probes shifted transversely by  $0.25w$  toward the edge of the waveguide. From Fig. 7, we see that the odd modes are negligible when the probes are centered transversely, whereas the single-mode passband is halved for the off-center case. Further results not shown here reveal that the

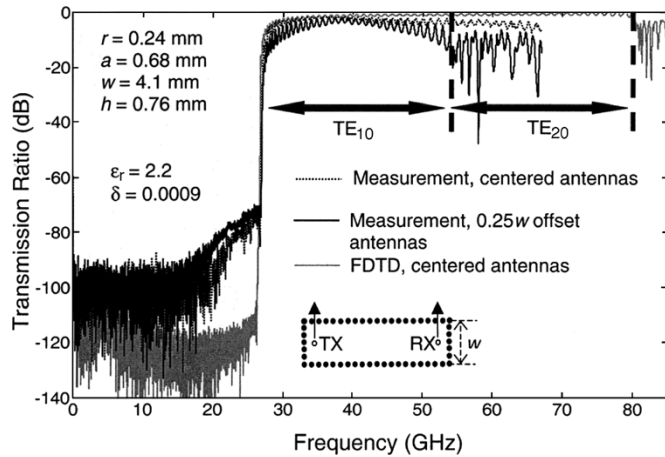


Fig. 7. Comparison of the measured  $S_{21}$  characteristics for 7.6-cm-long SIW interconnects of the type shown in Fig. 4 for the case of both transmitting and receiving probes at the optimum transverse and longitudinal locations, and for the case of both probes shifted transversely by  $0.25w$  toward the edge of the waveguide. To illustrate the full width of the passband for the centered case beyond the limitations of the 67-GHz network analyzer, the FDTD-calculated insertion loss for the centered case is also shown.

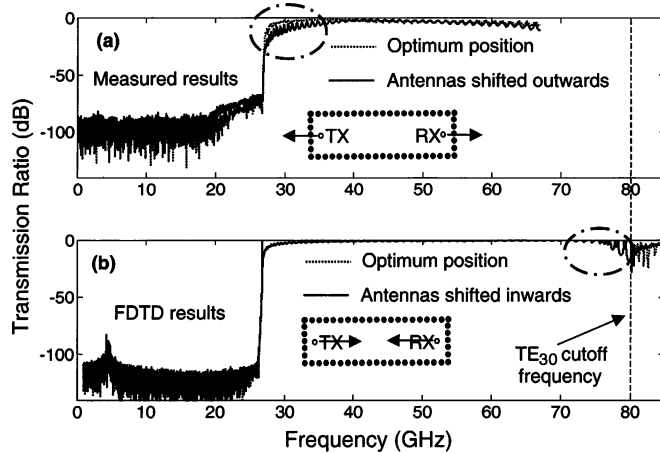


Fig. 8. Comparison of the  $S_{21}$  characteristics for 7.6-cm-long SIW interconnects of the type shown in Fig. 4, one having transmitting and receiving probes at the optimum transverse and longitudinal locations, and one having both probes: (a) shifted longitudinally outwards toward the end of the waveguide by  $1.5r$  and (b) shifted longitudinally inwards toward the center of the waveguide by  $1.5r$ . We highlight with superimposed circles the effect on the bandwidth from shifting the probes.

much smaller transverse deviations of the probes from the center line caused by typical manufacturing tolerances generate an acceptably low level of odd modes. Hence, it appears feasible to manufacture SIW interconnects having passbands that extend from the cutoff frequency of the fundamental TE mode to the cutoff frequency of the second even TE mode, yielding  $\sim 100\%$  relative bandwidth.

We now discuss reason 2) for the improved bandwidth of the SIW structures discussed here relative to our previous results: optimized longitudinal probe placement. Fig. 8 illustrates the effect of moving the transmitting and receiving probes longitudinally relative to the optimum position by  $1.5r$ . Compared to the optimum case, we find that the  $S_{21}$  characteristic at the lower end of the passband is degraded for probes shifted closer

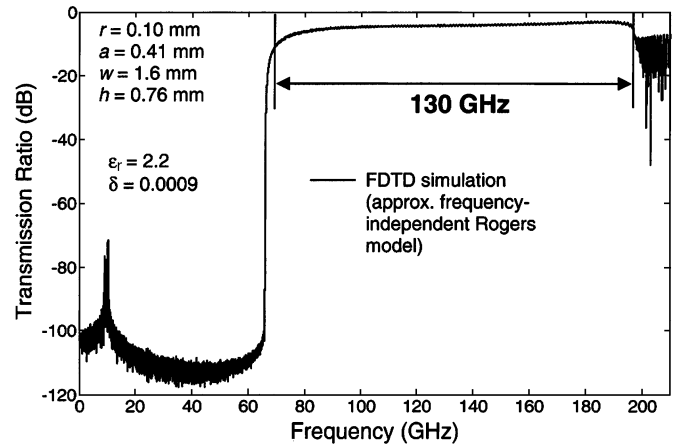


Fig. 9. FDTD-calculated  $S_{21}$  characteristic over a 7.6-cm-long SIW interconnect analogous to that shown in Fig. 4, but scaled to a center frequency of 130 GHz.

to the waveguide ends [see Fig. 8(a)]. Furthermore, destructive interference degrades the  $S_{21}$  characteristic at the upper end of the passband for probes shifted away from the waveguide ends [see Fig. 8(b)].

Our final single straight SIW structure under study is one scaled to a center frequency of 130 GHz. This example serves to illustrate the scalability of the SIW technology to center frequencies well above 100 GHz (reaching as high as 200 GHz with no required improvements in circuit board manufacturing techniques). The SIW structure of interest spans 0.76 mm between the upper and lower ground planes and has  $r = 0.10$  mm, and  $a = 0.41$  mm and  $w = 1.6$  mm. Fig. 9 shows the FDTD-calculated  $S_{21}$  characteristic of this device, assuming a frequency-independent model for the Rogers RT/Duriod 5880 dielectric. Here, we see that an  $\sim 100\%$  relative-bandwidth passband exists between 65 and 195 GHz, which is suitable for data rates well exceeding 100 Gb/s. In ongoing research, this structure is being fabricated and tested in the laboratory.

## V. CROSSTALK STUDY

Our new computational and experimental results for crosstalk between adjacent SIWs is presented here. Two waveguides of the type shown in Fig. 4 are arranged to share a row of pins along a common sidewall, as shown in the insets of Fig. 10(a) and (b). We consider two modes of crosstalk: from TX to XT1 in a direction normal to the common sidewall; and from TX to XT2, representing a longitudinal coupling of the two waveguides. Each waveguide's dimensions are equivalent to the 50-GHz center-frequency waveguide considered in Section IV (pin radius  $r = 0.24$  mm, pin center-to-center spacing  $a = 0.68$  mm, waveguide width  $w = 4.1$  mm, waveguide height  $h = 0.76$  mm, and 0.20-mm gaps between adjacent pins). Excitation is provided at TX by the same 134-ps 50-GHz carrier pulse described earlier in Section IV.

Fig. 10(a) and (b) shows the FDTD-calculated crosstalk voltage time waveforms at XT1 and XT2, respectively. These waveforms are normalized relative to the maximum received voltage time-waveform value at RX. We see that the peak crosstalk voltages at XT1 and XT2 are on the order of 0.02%

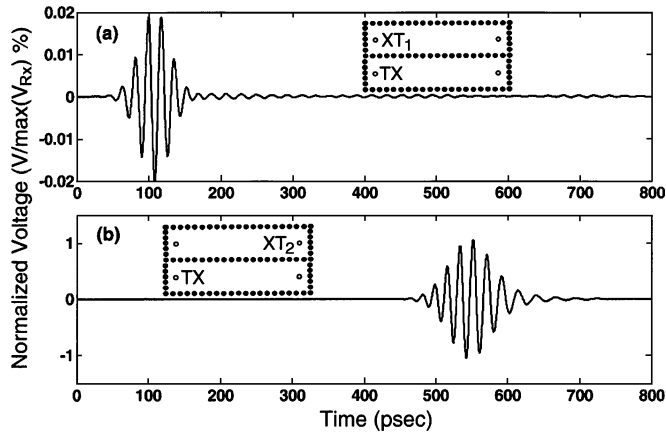


Fig. 10. FDTD-calculated crosstalk voltage time-waveforms at: (a) XT1 and (b) XT2. These waveforms are for an assumed 134-ps (full-width at half-maximum) transmitted 50-GHz carrier pulse having a Gaussian envelope, and are normalized relative to the maximum received voltage time-waveform value at RX.

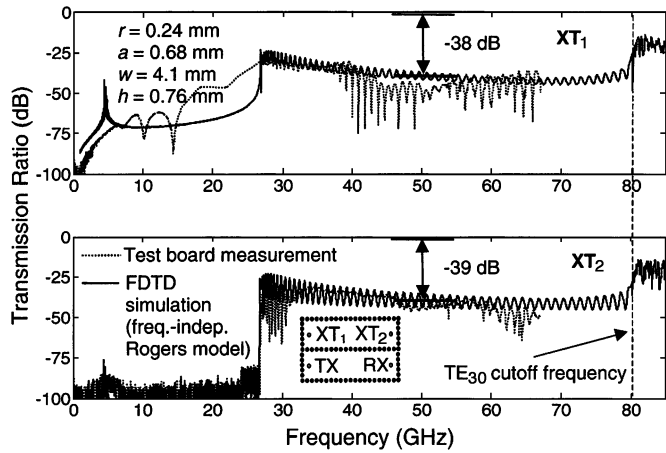


Fig. 11. Comparison between the measured and FDTD-calculated crosstalk for two adjacent 7.6-cm-long SIW interconnects of the type shown in Fig. 4. For both XT 1 and XT 2, the crosstalk level is below  $-30$  dB, wherein 0.20-mm gaps exist between the adjacent vias having  $r = 0.24$  mm.

and 1%, respectively, relative to the peak voltage of the desired received signal.

Fig. 11 shows the associated spectrum of the measured and FDTD-calculated crosstalk between the SIWs of Fig. 10. We see that, for pin-to-pin gaps on the order of 42% of the size of each pin, one row of pins can suppress the worst case crosstalk to below  $-30$  dB, which is well within tolerable levels for our application.

## VI. OPTIMIZED 45° AND 90° BENDS

FDTD modeling results for optimized 45° and 90° SIW bends capable of maintaining the ultrawide relative bandwidth of  $\sim 100\%$  are reported here. Here, we are interested in a design that minimally degrades the ultrawideband characteristics of the straight SIW structures considered in the previous sections. Our extensive studies have shown that, without careful placement of the vias in the vicinity of the bend, odd modes are generated, which reduce the single-mode passband by approximately 50%, in the manner seen in Fig. 7.

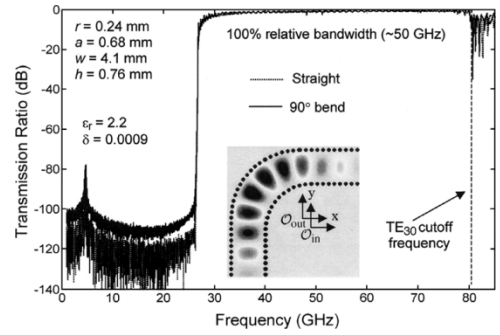


Fig. 12. Comparison between the FDTD-calculated  $S_{21}$  characteristics of the straight and 90° bend SIWs of the type shown in Fig. 4.

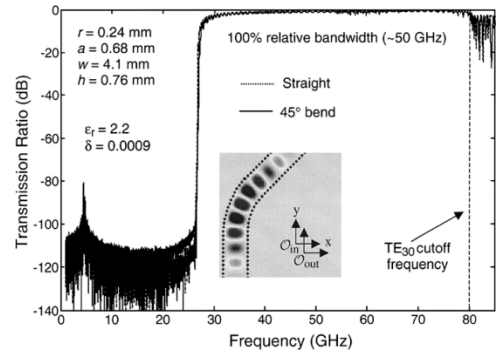


Fig. 13. Comparison between the FDTD-calculated  $S_{21}$  characteristics of the straight and 45° bend SIWs of the type shown in Fig. 4.

Fig. 12 illustrates our results for the most promising arrangement for a 90° bend. Here, the outer circular arc of vias has a 4.1-mm radius of curvature, while the inner circular arc has a 5.4-mm radius of curvature whose origin is displaced radially inward by 1.4 mm relative to the origin of the outer arc. These differences between the two sidewall arcs counteract the differing propagation lengths along the inside and outside edges of the bend. As seen in the graph of Fig. 12, there is very little difference between the calculated ultrawideband  $S_{21}$  characteristics for the optimized 90°-bend and a straight SIW having the same overall length. Furthermore, as shown in the inset of Fig. 12, there is little if any odd-mode generation even for the worst case of a propagating pulse localized within the bend.

Fig. 13 illustrates our results for the most promising arrangement for a 45° bend. Here, the outer elliptical arc of vias is described by  $x^2 + y^2/1.2 = 9.5$  mm, while the inner circular arc has an 8.2-mm radius of curvature whose origin is displaced radially outward by 1.4 mm relative to the origin of the outer arc. As seen in the graph of Fig. 13, there is very little difference between the calculated ultrawideband  $S_{21}$  characteristics for the optimized 45° bend and a straight SIW having the same overall length. Furthermore, as shown in the inset of Fig. 13, there is little if any odd-mode generation even for the worst case of a propagating pulse localized within the bend.

## VII. CONCLUSIONS AND ONGOING RESEARCH

This paper has reported an experimental and computational study of SIWs optimized for use as ultrahigh-speed band-pass waveguiding digital interconnects. Specifically, we have

shown how to design SIWs optimized for narrow transverse dimensions, low loss, low crosstalk, and maximum bandwidth with no multimoding. The novelty of this study resides in our successful design, fabrication, and testing of low-loss SIWs that achieve 100% relative bandwidths via optimal excitation of the dominant  $TE_{10}$  mode and avoidance of the excitation of the  $TE_{20}$  mode. Furthermore, these optimal structures maintain their 100% relative bandwidth while transmitting around  $45^\circ$  and  $90^\circ$  bends, and achieve measured crosstalk of better than  $-30$  dB over the entire passband. We have supported our computational designs with laboratory measurements of prototype SIWs that achieved  $\sim 100\%$  relative bandwidths at center frequencies of 50 GHz, accommodating in principle data rates of 50 Gb/s.

Since existing circuit-board technology permits dimensional reductions of SIWs by a factor of 4:1 relative to the ones discussed here, bandpass operation at center frequencies approaching 200 GHz with data rates of 200 Gb/s are feasible. These data rates meet or exceed those expected eventually for proposed optical interconnects without requiring the development of a suite of essentially revolutionary silicon photonic technologies.

As part of our future research, we will perform laboratory measurements on both the 130-GHz center frequency SIW of Fig. 9 and the  $45^\circ$  and  $90^\circ$  SIW bends of Figs. 12 and 13. We will also develop optimized bends for other angles. In addition, we will investigate the design of structures for frequency-division multiplexing/demultiplexing of multiple data channels onto a single SIW, as well as demonstrate working prototypes wherein SIWs are connected to actual Intel Corporation processors and memories.

#### ACKNOWLEDGMENT

The authors are pleased to recognize the support of B. Horine, Platform Technologies Laboratory, Intel Corporation, Hillsboro, OR, for his assistance in the design and manufacturing of the test samples.

#### REFERENCES

- [1] G. E. Moore, "Cramming more components onto integrated circuits," *Electronics*, vol. 38, no. 8, pp. 114–117, Apr. 1965.
- [2] S. Coffa, "Light from silicon," *IEEE Spectr.*, pp. 44–49, Oct. 2005.
- [3] J. Hirokawa and M. Ando, "Single-layer feed waveguide consisting of posts for plane TEM wave excitation in parallel plates," *IEEE Trans. Antennas Propag.*, vol. 46, no. 5, pp. 625–630, May 1998.
- [4] H. Uchimura, T. Takenoshita, and M. Fujii, "Development of a 'laminated waveguide'," *IEEE Trans. Microw. Theory Tech.*, vol. 46, no. 12, pp. 2438–2443, Dec. 1998.
- [5] F. Xu and K. Wu, "Guided-wave and leakage characteristics of substrate integrated waveguide," *IEEE Trans. Microw. Theory Tech.*, vol. 53, no. 1, pp. 66–73, Jan. 2005.
- [6] F. Capolino, D. R. Jackson, and D. R. Wilton, "Mode excitation from sources in two-dimensional SIW waveguides using the array scanning method," *IEEE Microw. Wireless Compon. Lett.*, vol. 15, no. 2, pp. 49–51, Feb. 2005.
- [7] A. Zeid and H. Baudrand, "Electromagnetic scattering by metallic holes and its applications in microwave circuit design," *IEEE Trans. Microw. Theory Tech.*, vol. 50, no. 4, pp. 1198–1206, Apr. 2002.
- [8] L. Yan, W. Hong, K. Wu, and T. J. Cui, "Investigations on the propagation characteristics of the substrate integrated waveguide based on the method of lines," *Proc. Inst. Elect. Eng.—Microw., Antennas, Propag.*, vol. 152, no. 1, pp. 35–42, 2005.

- [9] F. Xu, K. Wu, and W. Hong, "Domain decomposition FDTD algorithm combined with numerical TL calibration technique and its application in parameter extraction of substrate integrated circuits," *IEEE Trans. Microw. Theory Tech.*, vol. 54, no. 1, pp. 329–338, 2006.
- [10] E. Yablonovitch, "Photonic bandgap structures," *J. Opt. Soc. Amer. B, Opt. Phys.*, vol. 10, pp. 283–295, 1993.
- [11] J. D. Joannopoulos, R. D. Mead, and J. N. Winn, *Bandgap Structures: Molding the Flow of Light*. Princeton, NJ: Princeton Univ. Press, 1995.
- [12] J. J. Simpson, A. Taflove, J. A. Mix, and H. Heck, "Computational and experimental study of a microwave electromagnetic bandgap structure for potential use as a bandpass wireless interconnect," *IEEE Microw. Wireless Compon. Lett.*, vol. 14, no. 7, pp. 343–345, Jul. 2004.
- [13] ———, "Advances in hyperspeed digital interconnects using electromagnetic bandgap technology: Measured low-loss 43-GHz passband centered at 50 GHz," in *Proc. IEEE AP-S Int. Symp.*, Washington, DC, Jul. 2005, pp. 26–29.
- [14] M. Piket-May, W. K. Gwarek, T.-L. Wu, B. Houshmand, T. Itoh, and J. J. Simpson, "High-speed electronic circuits with active nonlinear components," in *Computational Electrodynamics: The Finite-Difference Time-Domain Method*, A. Taflove and S. C. Hagness, Eds., 3rd ed. Norwood, MA: Artech House, 2005.
- [15] A. Taflove and S. C. Hagness, *Computational Electrodynamics: The Finite-Difference Time-Domain Method*, 3rd ed. Norwood, MA: Artech House, 2005.
- [16] ———, "No exponential is forever: But 'forever' can be delayed," in *IEEE Solid-State Circuits Conf. Tech. Dig.*, San Francisco, CA, Feb. 2003, vol. 1, pp. 20–23.
- [17] J. H. Sinsky, M. Duelk, and A. Adamiecki, "High-speed electrical backplane transmission using duobinary signaling," *IEEE Trans. Microw. Theory Tech.*, vol. 53, no. 1, pp. 152–160, Jan. 2005.
- [18] M. Celuch-Marcysiak, W. K. Gwarek, and M. Sypniewski, "A simple and effective approach to FDTD modeling of structures including lossy metals," in *Proc. Asia-Pacific Microw. Conf.*, Yokohama, Japan, Dec. 1998, pp. 991–993.
- [19] S.-K. Fan, J.-A. Paik, P. Patterson, M. C. Wu, B. Dunn, and C.-J. Kim, "MEMS with thin-film aerogel," in *IEEE Microelectromech. Syst. Conf.*, Interlaken, Switzerland, Jan. 2001, pp. 122–125.



**Jamesina J. Simpson** (S'01) was born in Portsmouth, VA, on July 20, 1981. She is currently working toward the Ph.D. degree in electrical engineering at Northwestern University, Evanston, IL.

Since her freshman undergraduate year, she has been a Research Assistant with the Computational Electromagnetics Laboratory, Northwestern University. Her current research interests include FDTD modeling of geophysically induced extremely low-frequency propagation about the entire Earth and FDTD modeling of novel ultrahigh-speed

bandpass wireless interconnects for next-generation digital circuits.

Ms. Simpson is a member of Tau Beta Pi. She was the recipient of the National Science Foundation Graduate Research Fellowship and the Walter P. Murphy Fellowship for her graduate studies.



**Allen Taflove** (F'90) has been a Professor with the Department of Electrical Engineering and Computer Science, Northwestern University, Evanston, IL, since 1984. Since 1972, he has pioneered basic theoretical approaches and engineering applications of FDTD computational electrodynamic. In a 1980 IEEE paper, he coined the FDTD acronym. He has authored or coauthored five books, 20 book chapters and papers, over 100 refereed journal papers, and 300 conference papers. He holds 14 U.S. patents. His research interests span much of the electromagnetic

spectrum. He and his students model electrodynamic phenomena ranging from geophysically induced ultralow-frequency wave propagation about the entire Earth to the light-scattering behavior of early-stage colon cancer cells. The principle that "Maxwell's equations work from dc to light" and especially for the benefit of human society is demonstrated in his laboratory every day. His publications have resulted in his being included on ISIHighlyCited.com, the Institute of Scientific Information's list of the most-cited researchers worldwide. He has been the adviser or co-advisor of 20 Ph.D. recipients and one

post-doctoral fellow, five of whom are now tenured or tenure-track university professors.

Prof. Taflove is currently an elected member of Northwestern's General Faculty Committee. He is also the faculty advisor to the Undergraduate Design Competition, the Honors Program in Undergraduate Research, and the student chapters of Eta Kappa Nu and Tau Beta Pi. His efforts on behalf of students at all levels were recognized by Northwestern in 2000, when he was named a Charles Deering McCormick Professor of Teaching Excellence.



**Jason A. Mix** received the B.S. degree in electrical engineering from the Rose-Hulman Institute of Technology, Terre Haute, IN, in 1993, and the M.S. and Ph.D. degrees in electrical engineering from the University of Colorado at Boulder, in 1995 and 1999 respectively.

Upon graduation, he joined the Intel Corporation, Hillsboro, OR, where he is currently a Staff Hardware Engineer. His research interests include the field of microwave and millimeter-wave passive devices and high-speed digital interconnect design.



**Howard Heck** (M'04) earned the B.S.Ch.E. degree from Northwestern University, Evanston, IL, in 1985, and the M.S.E.E. degree from the National Technological University, Fort Collins, CO, in 1994.

From 1985 to 1995, he was with IBM, where he developed high-performance PCB and chip packaging technologies including HyperBGA technology. Since joining the Intel Corporation, Hillsboro, OR, in 1995, he has focused on research and development for high-speed inter-chip interconnects. He led the development team for the Pentium

II 100-MHz Frontside Bus, and managed teams which developed technology solutions for Direct RDRAM, DDR II, Pentium 4 Processor Frontside Bus, and Accelerated Graphics Port (AGP) interfaces. He currently leads a research and development team with the Corporate Technology Group, Intel Corporation, which is focused on modeling, simulation, measurement, and technology development for 10+–Gb/s signaling. Since 1997, he has also held a position as an Adjunct Professor with the Oregon Graduate Institute, Beaverton, where he teaches high speed digital interconnect design. He holds five U.S. patents with four pending.

Mr. Heck was the recipient of an Intel Corporation Achievement Award.